Circularly polarized absorption and luminescence of semiconductor Eu-OCN nanocrystals in blue light region

Yasuchika Hasegawa, Katsumasa Koide, Makoto Tsurui, Yuichi Kitagawa, Takayuki Nakanishi, Yoshihiro Doi, Yukio, Hinatsu and Koji Fushimi*

Prof. Y.Hasegawa, Dr. Y. Kitagawa
Institute for Chemical Reaction Design and Discovery (WPI-ICReDD), Hokkaido University, Sapporo, Hokkaido 001-0021, Japan
E-mail: hasegaway@eng.hokudai.ac.jp

K. Koide, M.Tsurui, K. Fushimi
Faculty of Engineering, Hokkaido University, N13 W8, Kita-ku, Sapporo, Hokkaido 060-8628, Japan

T. Nakanishi
Research Center for Functional Materials, National Institute for Materials Science, 1-1, Namiki, Tsukuba, 305-0044, Japan

Dr. Y. Doi, prof. Hinatsu
Faculty of Science, Hokkaido University, N10 W8, Kita-ku, Sapporo, Hokkaido 060-8628, Japan

Keywords: Europium, semiconductor, nanocrystal, Circularly polarized luminescence

Semiconductor nanomaterials with efficient polarized-light control in the blue region of the visible spectrum are promising candidates for modern and future photo-information technology, display devices, and optical sensing applications. New-type semiconductor $Eu(OCN)_2$ nanocrystals with circularly polarized absorption (CD: circular dichroism) and emission (CPL: circularly polarized luminescence) under an applied magnetic field here demonstarted for the first time. The effective CD signal at 1.6 T was observed at approximately 440 nm. The dissymmetry factor of CPL under 100 K, $g_{M\text{-}CPL,}$ was estimated to be 0.01. These characteristic circularly polarized absorption and emission phenomena of $Eu(OCN)_2$ nanocrystals should be caused by combination between the "*Faraday A* and *C terms"* of the magnetic moment in the excited state. Polarized-light control using $Eu(OCN)_2$ nanocrystals in the blue-light region is a large first step into a new world of photo-functional semiconductor nanomaterials.

Polarized-light control using optomagnetic materials opens advanced and frontier fields of photo-information science and technology.[1] Optomagnetic materials with polarized absorption control, i.e., the Faraday rotation effect, are important for the development of optical isolators for high-power coherent lasers and fiber-optic telecommunication systems.[2] This effect induces polarized absorption by a material in response to an applied external magnetic field. Optical telecommunication switching systems, circulators and imaging sensors based on Faraday devices have been used in industrial applications.[3] In the fields of photonics and medical engineering, control of polarized light in the visible wavelength region is desirable for VLC (visible-light communication) and optical visible sensors.[4] Although the circularly polarized luminescence (CPL) of optomagnetic materials has not been reported, various types of chiral luminescent molecules with natural-CPL have been described.[5] Effective optomagnetic materials with magnetic-CPL in the visible region are also expected to be useful in photonic applications such as future three-dimensional displays and advanced photo-security system.[6] Optomagnetic materials with polarized-light control in the visible region under magnetic field are required for advanced photonic science and engineering.

In efforts to develop opto-magnetic materials with applications in the visible-light region, researchers have explored lanthanide inorganic materials with magnetic *4f* spin configuration. Optical glass containing paramagnetic Tb(III) ions has recently been used in optical isolators that operate in the visible region.[7] Single crystals and ceramics of TGG ($Tb_3Ga_5O_{12}$), TAG ($Tb_3Al_5O_{12}$), TSLAG ($Tb_3Sc_{2-x}Lu_xAl_3O_{12}$) with Tb(III) ions have been also reported.[8] The Faraday effect on these Tb(III) compounds is based on their weak *4f-5d* electronic transitions, resulting in a low Faraday effect efficiency ($7^o\ cm^{-1}$ at 633 nm, 0.1 T).[7-9] The large *4f-5d* electronic transition of magnetic lanthanide materials would provide effective Faraday and CPL effects in the visible region. We have studied on semiconductor Eu(II) chalcogenides (EuS and EuSe) nanocrystals, which exhibit large *4f–5d* electronic allowed transitions that

enable effective Faraday rotation in the visible region.[11] The Faraday rotation wavelength can be fine-tuned by controlling the crystal size (quantum size effect). Stoll and Jin also studied enhancement of the Curie temperature of nano-sized Gd(III)-doped EuS.[12] EuS-Au nano-systems have also investigated in photoinduced-Faraday switching devices based on the plasmonic technology.[13] Thus, the Eu(II) chalcogenides are promising candidates for use in devices that enable magnetic optical activity control in the visible region.

Previous Eu(II) chalcogenides with polarized-light control are suitable for red-light optical pathways (600-750 nm). The development of novel Eu(II) chalcogenides with polarized-light control in the blue-light region (< 500 nm), likely requires an Eu(II) compound with a large-energy-gap *4f-5d* transition. Here, we focused on recent nephelauxetic studies on Eu(II) compounds.[14] The energy gap of the *4f-5d* transition of Eu(II) is influenced by the coordination structure and geometry, which are in turn dependent on the counter anions. Due to the nephelauxetic effect, the energy gap of an Eu(II) material composed of Eu(II)-O bonds is larger than the gap of materials composed of Eu(II)-S and Eu(II)-Se bonds. The EuO nanomaterials also emit a photon under excitation at their *4f-5d* transition bands.[15] For luminescent semiconductor nanomaterials composed of Eu(II)-O bonds (Eu(II)-O nanomaterials), the electronic configuration of the excited state (*5d* band) differs substantially from that of the ground state (degenerated 4f orbitals), promoting circularly polarized absorption (circular dichroism: CD) and emission (circularly polarized luminescence: CPL) phenomena under photo-irradiation. However, in previous studies, EuO nanocrystals have been found to be unstable under air, resulting in the formation of europium(III) oxides (Eu_2O_3) on the nanocrystal surface.[16] The development of novel air-stable and luminescent Eu(II)-O nanomaterials is a key point for opening a new field of optical polarized-light-control devices with blue light sources. In the present study, air-stable and novel $Eu(OCN)_2$ nanocrystals with circularly polarized-light control (absorption and emission) in the blue wavelength range (350-500 nm) are demonstrated under magnetic field.

The previously reported synthesis of EuS and the synthesis of the novel $Eu(OCN)_2$ are illustrated in Figure 1. In a previous study, we prepared EuS nanocrystals by partial oxidation of an Eu metal ingot with thiourea ($S=C(NH_2)_2$) in liquid ammonia solution (Figure 1a).[11a] The ammonia promotes dissolution and oxidation of the Eu metal, resulting in smooth formation and protection of Eu(II) ions in the system. On the basis of this reaction, we here attempted to synthesize Eu(II)-O nanocrystals using an oleylamine solution containing urea ($O=C(NH_2)_2$) molecules under heat treatment (Figure 1b). The heat treatment of the oleylamine solution containing Eu metal and urea produced a yellow powder.

The prepared yellow powder was characterized by infrared (IR) spectroscopy and X-ray diffraction (XRD). A characteristic signal of the OCN^- anion signal in the IR spectrum was observed at around ~2200 cm^{-1} (Supporting Information Figures S1a-ii). The *2θ* diffraction peaks at 11.46, 13.90, 18.67, 20.67, 23.04, 23.19, 24.86, 24.96, 27.54, 27.88, 28.92, 30.74, 31.14, and 31.88º in the XRD patterns agree well with those of the corresponding (100), (002), (012), (11-2), (200), (112), (020), (120), (21-2), (121), (014), (11-4), and (122) diffraction planes of the Eu(II) compound with two OCN^- ions and one urea molecules, $Eu(OCN)_2(OC(NH)_2)$ ($Eu(OCN)_2$-urea), respectively (Figures 2a-i: black line). The reaction is expressed as,

$$OC(NH)_2 \rightarrow NH_4 + OCN^- \quad (1)$$

$$Eu(0) + OC(NH)_2 + 2NH_4^+ + 2OCN^- \rightarrow Eu(OCN)_2(OC(NH)_2) + NH_3 + H_2 \quad (2).$$

In these reactions, oleylamine molecules play an important role in effectively protecting the crystal surface of $Eu(OCN)_2$-urea, functioning such as a surfactant in solution. The DSC thermogram of the prepared yellow $Eu(OCN)_2$-urea powder shows endothermic signals, and its TGA trace shows a weight-loss at approximately 220 ºC, respectively (TGA: Supporting Information Figures S1a-i; DSC: Figures S1a-ii). These thermal analyses indicate that structural transformation from $Eu(OCN)_2$-urea to other Eu compounds occurs under heat treatment at ~220 ºC.

After heat treatment of $Eu(OCN)_2$-urea powder at 220 ºC, we obtained a pale-yellow powder whose IR spectrum shows no N-H vibrational signals on IR measurement (Supporting Information Figures S1a-ii). The *2θ* XRD peaks of the pale-yellow powder at 18.04, 21.76, 28.01, 31.67, 32.80, 33.15, 36.07, 41.67, 43.34, 45.46, 46.25, 47.74, 48.94, and 51.29º are assigned to the (111), (022), (113), (040), (202), (220), (133), (115), (151), (224), (242), (135), (026), and (331) planes of $Eu(OCN)_2$, respectively (Figures 2a-ii: red line, These XRD data well-agree with those for bulk $Eu(OCN)_2(OC(NH)_2)$ and $Eu(OCN)_2$.[17]). This simple transformation is given by,

$$Eu(OCN)_2(OC(NH)_2) \rightarrow \quad Eu(OCN)_2 + OC(NH)_2 \quad (3).$$

In the $Eu(OCN)_2$ crystals, Eu(II) ions are coordinated with O and N atoms in OCN^- anions. The elimination of urea in bulk $Eu(OCN)_2$-urea at 200 ºC and formation of $Eu(OCN)_2$ have been also reported.[17] Generally, ammonium cyanate is unstable, resulting in transformation to urea at 60oC, easily. Combination of Eu(0), urea and oleylamine is suitable for formation of $Eu(OCN)_2$ nanocrystals.The coordination geometry of $Eu(OCN)_2$ is categorized as an eight-coordinated pseudo square-anti prism structure, which differs substantially from the coordination structures of EuO and EuS crystals (cubic structure). TEM images of $Eu(OCN)_2$-urea and $Eu(OCN)_2$ powders are shown in Figures 2b and c, respectively (high-res image of $Eu(OCN)_2$-urea, see supporting imformation Fig. S2). Characteristic rod-shaped $Eu(OCN)_2$-urea and rugged $Eu(OCN)_2$ nanocrystals are observed. The average lengths of the short (width) and long (length) axes of the $Eu(OCN)_2$-urea crystals were estimated from the TEM images to be 27 nm and 133 nm, respectively (Figure 2d). The single-source precursor $Eu(OCN)_2$-urea nanorods promote the formation of nano-sized $Eu(OCN)_2$ crystals at 220 ºC. The average particle size of $Eu(OCN)_2$ was found to be 39 nm (Figure 2e), which is the same as the crystal grain sizes calculated from the XRD pattern using Scherrer's equation (38 nm). The superparamagnetic properties of $Eu(OCN)_2$ and precursor $Eu(OCN)_2$-urea nanocrystals were also characterized using a superconducting quantum interface device (SQUID)

measurements (Supporting information Figsures S3 and S4). We speculate that the crystal-transformation of $Eu(OCN)_2$-urea nanorods at 220ºC is a key factor for the successful formation of $Eu(OCN)_2$ nanocrystals without including crystal-aggregation and -necking processes among nanocrystals (Figure 3). Thus, $Eu(OCN)_2$ nanocrystals were prepared for the first time.

Prepared $Eu(OCN)_2$ and $Eu(OCN)_2$-urea nanocrystals exhibit luminescence at 100 K and 90 K, respectively, as shown in Figure 4a. The characteristic emission bands of the $Eu(OCN)_2$ nanocrystals are observed at approximately 480 nm (blue emission: red line, inset Figure 4a-i), which is assigned to the *4f-5d* ($4f^7(^8S_{7/2})$-$4f^6(^7F_J)5d^1(t_{2g}, e_g)$) transition of a Eu(II) ion. The wavelengths of the emission and excitation bands of the $Eu(OCN)_2$ nanocrystals are shorter than those of the precursor $Eu(OCN)_2$-urea nanocrystals (green emission: black line, inset Figure 4a-ii). The blue shift of the emission and excitation bands of the $Eu(OCN)_2$ nanocrystals might stem from diminished crystal field upon elimination of the n-π* transition of urea molecules in the Eu(II) coordination sphere. These excitation spectra are similar to diffuse relectance spectra of $Eu(OCN)_2$ and $Eu(OCN)_2$-urea powders (see supporting information Fig. S6). The emission decay profiles are shown in Figure 4b. The time-resolved emission profile produced by precursor $Eu(OCN)_2$-urea nanorods at 100 K exhibits double-exponential decays, with nanosecond-scale lifetimes, as shown in Figure 4b (black line). The emission lifetimes were determined from the slopes of logarithmic plots of the decay profiles. The two components of the emission lifetimes for $Eu(OCN)_2$-urea were estimated as 40 and 107 ns. These nano-scale and double-exponential decay curves are attributed to the presence of two types of luminescent Eu(II) ions in the nanocrystals. By contrast, the time-resolved emission profile produced by $Eu(OCN)_2$ nanocrystals at 90 K shows triple-exponential decays (Figure 4b, red line). The three components of the emission lifetimes for $Eu(OCN)_2$ nanocrystals were calculated to be 18 ns, 54 ns, and 150 ns. Their three emission centers in Eu(II) nanocrystals may originate from the surface and internal luminescence, respectively.

The photophysical properties of $Eu(OCN)_2$ are based on the stable formation of the excited state ($4f^6(^7F_J)5d^1(t_{2g}, e_g)$) under photo-irradiation. We previously reported a luminescence spectrum (λ_{max} = 357 nm) of EuO nanocrystals under irradiation.[15] By contrast, the excited spin of EuS materials under irradiation thermally relaxes to the ground state, resulting in non-emission. The energy gap in the Eu-O lattice is much larger than that in the Eu-S lattice due to the nephelauxetic effect on Eu(II) compounds.[16] We consider that the larger energy gaps of $Eu(OCN)_2$ nanocrystals suppress their phonon-relaxation in a crystal lattice, and enhance the luminescence properties at 100 K. The emission lifetimes of $Eu(OCN)_2$ nanocrystals are temperature dependent. The emission decays times decrease with increasing temperature ($Eu(OCN)_2$: 16 ns and 57 ns at 100K). The temperature-dependent emission might be caused by a quenching pathway such as an electron deep trap-site in the conduction band.[18] At the present stage, the $Eu(OCN)_2$ surface is not protected using a specific organic surfactant, polymer, or surface-modified reagent. Effective surface protection of semiconductor nanomaterials promotes strong luminescence at room temperature.[19] Study on the surface protection of semiconductor $Eu(OCN)_2$ nanocrystals might be an important factor for the development of future photonic nanomaterials.

Polymethylmethacrylate (PMMA) disks containing $Eu(OCN)_2$ nanocrystals were prepared for measurements of circularly polarized absorption (CD) and emission (CPL) (Figure 5a). The prepared PMMA disk with $Eu(OCN)_2$ nanocrystals is a high-transparency material in the UV- and visible-light regions, whereas the PMMA disks with EuS nanocrystals exhibits a purple color. The CD spectrum at room temperature and under an applied field of 1.6 T exhibited clear positive and negative peaks; this effect might have contributed to the *4f-5d* transitions of the Eu(II) nanocrystals. The wavelength of the positive peak for $Eu(OCN)_2$ (λ_{max} = 420 nm, Fgure 5b black line) nanocrystals is effectively blue-shifted compared with that of the EuS (λ_{max} = 640 nm) nanocrystals (Figure 5b red line). Faraday rotation angle is related to the

dissymmetry factor on circularly polarized absorption (CD) spectra in magnetic field, $g_{M\text{-}CD}$. The calculated $g_{M\text{-}CD}$ constants are summarized in Table 1. The dissymmetry factor for $Eu(OCN)_2$-urea ($g_{M\text{-}CD}$ = 0.0055) and $Eu(OCN)_2$ ($g_{M\text{-}CD}$ = 0.0063) disks are smaller than that of the EuS disk ($g_{M\text{-}CD}$ = 0.0253).

The CPL of the $Eu(OCN)_2$ disk at 1.6 T and 100 K is shown in Figure 5c. We observed CPL signals for the PMMA disk with $Eu(OCN)_2$ nanocrystals. This result is the first observation of a magnetic CPL of luminescence semiconductor nanocrystals. The magnetic CPL spectral shape of the $Eu(OCN)_2$ PMMA-disk (blue luminescence at 100 K, Figue 5c inset) in Fig. 5c well agrees with the emission spectrum of $Eu(OCN)_2$ powder in Fig. 4a (red line). The first magnetic CPL should arise from the *5d-4f* transition in semiconductor $Eu(OCN)_2$ nanocrystals. The dissymmetry factors $g_{M\text{-}CPL}$ of $Eu(OCN)_2$ and $Eu(OCN)_2$-urea disks were found to be approximately 0.01 and 0.001, respectively. The Magnetic CD and CPL effects are clarified into three terms, *Faraday A* (degenerated excited state), *B* (perturbation of magnetic dipole moment) and *C* (degenerated ground state).[20] The CPL of Eu(II) compounds should be generally caused by *Faraday C* term on $4f^7$ configuration under magnetic field. Notably, the magnetic behavior of $Eu(OCN)_2$ nanocrystals (magnetic moment in the ground state) is much more similar to that of the $Eu(OCN)_2$-urea nanocrystals in our experiments. Their magnetic moments are based on the concentration of Eu(II) ions in the crystals. The magnetic moment of the excited state should be influenced by the *5d* orbital, depending on the crystal field. We consider that superparamagnetic $Eu(OCN)_2$ crystals with large energy gap might promotes effective Stark and Zeeman effects on a large-splitting *5d* band under a magnetic field. The magneto-induced CPL of $Eu(OCN)_2$ crystals may be caused by combination between the *Faraday A* (degenerated excited state) and *C* (degenerated ground state) terms of the semiconductive magnetic moment in the excited state. The g_{CPL} of $Eu(OCN)_2$ nanocrystals is 10 times larger than that of $Eu(OCN)_2$-urea nanocrystals. We observed that the multi-component emission lifetime of $Eu(OCN)_2$ nanocrystals (54 and 150 ns) was larger than that of

$Eu(OCN)_2$-urea crystals (40, 107 ns). The larger g_{CPL} might be caused by stability of excited state of Eu(II) ions in nanomaterials, which is related to the Faraday *A*.

We successfully observed CPL of semiconductor $Eu(OCN)_2$ nanocrystals under an applied magnetic field at temperatures under 100 K. This work presents the first report of magnetic-field-induced CPL of semiconductor nanocrystals, although a magnetic-field-induced CPL of luminescent Eu(III) complexes and phthalocyanine compounds in liquid media have been previously reported.[21] The $Eu(OCN)_2$ nanocrystals were prepared by the reaction of an Eu ingot with urea in oleylamine under mild environmental conditions. Surface protection of $Eu(OCN)_2$ nanocrystals might be a key factor in improving their luminescence and magnetic CPL performance at room temperature. In this case, the results presented here could open a new fundamental path to the development of future opto-magnetic devices such as novel optical switching, sensing, and spintronic devices. The findings present here, being directly related to photophysical chemistry and future photo-functional materials science research, may provide new insights into the design of next-generation nanomaterials and may lead to the development of a novel area of study within the field of polarized-light science and technology.

Supporting Information
Supporting Information is available from the Wiley Online Library or from the author.

Acknowledgements
This work was supported by JSPS KAKENHI Grant Number JP18H04497. This work was also partially supported by two Grants-in-Aid for Scientific Research (18H02041, 20H02748, 20H04653, 20H05197).

Received: ((will be filled in by the editorial staff))
Revised: ((will be filled in by the editorial staff))
Published online: ((will be filled in by the editorial staff))

References

[1] a) N. Stafford, *Nature* **2010**, *467*, S19; b) L. Bi, J. Hu, P. Jiang, D.-H. Kim, G.F.Dionne, C. L. Kimerling, C. A. Ross, *Nature Photonics* **2018**, *5*, 758; c) E. R. Simpson, J. Mauritsson, *Nature Photonics* **2018**, *12*, 316.

[2] P.N. Schatz, A.J. McCaffery *Rev. Chem. Soc.* **1969**, *23*, 552.

[3] D. Jalas, A. Petrov, M. Eich, W. Freude, S. Fan, Z. Yu, R. Baets, M. Popović, A. Melloni, J. D. Joannopoulos, M. Vanwolleghem, C. R. Doerr, H. Renner, *Nature Photonics* **2013**, *7*, 579.

[4] a) J. An, Q. N. Pham, W.-Y. Chung, *Opt. Express* **2017**, *25,* 25477; b) H. Chun, A. Gomez, C. Quintana, W. Zhang, G. Faulkner, D. A. O'Brien, *Sci. Rep.* **2019**, *9*, 4952; c) Y.-W. Cheong, X.-W. Ng, W.-Y. Chung, *IEEE Sens. J.* **2013**, *13*, 3347.

[5] a) G. Muller, *Dalton Trans.* **2009**, 9692; b) R. Carr, N. H. Evans, D. Parker, *Chem. Soc. Rev.* **2012**, *41*, 7673, c) F. Zinna, L. Di Bari, *Chirality* **2015**, *27*, 1.

[6] Y. T. Sang, J. L. Han, T. H. Zhao, P. F. Duan, M. H. Liu, *Adv. Mater*. **2019**, 1900110.

[7] G. Gao, A. Winterstein-Beckmann, O. Surzhenko, C. Dubs, J. Dellith, M. A. Schmidt, L. Wondraczek, *Sci. Rep.* **2015**, *5*, 8942.

[8] Z. Chen, L. Yang, X. Wang, J. Wang, Y. Hang, *Opt. Mater.* **2015**, *46*, 12.

[9] Q. Hu, Z. Jia, Y. Yin, W. Mu, J. Zhang, X. Tao, *J. Alloys Compd.* **2019**, *805*, 496.

[11] a) T. Kataoka, Y. Tsukahara, Y. Hasegawa, Y. Wada, *Chem. Commun.* **2005**, 6038; b) Y. Hasegawa, T. Adachi, A. Tanaka, M. Afzaal, P. O'Brien, Y. Doi, Y. Hinatsu, K. Fujita, K. Tanaka, T. Kawai, *J. Am. Chem. Soc.* **2008**, *130,* 5710.

[12] a) M. D. Regulacio, K. Bussmann, B. Lewis, S. L. Stoll, *J. Am. Chem. Soc.* **2006**, **128**, 11173; b) R. S. Selinsky, J. H. Han, E.A. Morales Pérez, I. A. Guzei, S. Jin, S. *J. Am. Chem. Soc.* **2010**, *132,* 15997.

[13] A. Kawashima, T. Nakanishi, T. Shibayama, S. Watanabe, K. Fujita, K. Tanaka, H. Koizumi, K. Fushimi, Y. Hasegawa, *Chem. Eur. J.* **2013**, *19*, 14438.

[14] a) T. Wu, A. Ishikawa,T. Honda, H. Tamatsukuri, k. Ikeda, T. Otomo, S. Matsuishi, *RSC Adv.* **2019**, **9**, 5282; b) G. J. Hoerder, M. Seibald, D. Baumann, T. Schröder, S. Peschke,

P.C. Schmid, T. Tyborski, P. Pust, I. Stoll, M.Bergler, C. Patzig, S.Reißaus, M. Krause, L. Berthold, T. Höche, D. Johrendt, H. Huppertz, *Nature Comm.* **2019**, *10*, 1824.

[15] Y. Hasegawa, S. Thongchant, Y. Wada, H. Tanaka, T. Kawai, T. Sakata, H. Mori S. Yanagida, *Angew. Chem. Int. Ed.* **2002**, *41*, 2073-2075.

[16] a) G. Bellocchi, G. Franzò, F. Iacona, S. Boninelli, M. Miritello, T. Cesca, F. Priolo, *Opt. Express* **2012**, *20,* 5501; b) E. Negusse, J. Holroyd, M. Liberati, J. Dvorak, Y. U. Idzerda, T. S. Santos, J. S. Moodera, E. Arenholz, *J. Appl. Phys.* **2006**, *99*, 08E507.

[17] S. Pagano, G. Montana,C. Wickleder,W. Schnick, *Chem. Eur. J.* **2009**, *15*, 6186.

[18] R. Bachmann, P. Wachter, *J. Appl. Phys.* **1969**, *40,* 1326.

[19] M. Miyano, S. Endo, H. Takenouchi, S. Nakamura, Y. Iwabuti, O. Shiino, T. Nakanishi, Y. Hasegawa, *J. Phys. Chem. C* **2014**, 118, 19778

[20] J. P. Riehl, F. S. Richardson, *J. Chem. Phys.* **1977**, *66*, 1988.

[21] a) F. S. Richardson, H.G. Brittain, *J. Am. Chem. Soc.* **1981**, *103***,** 18; b) R. Schultheiss, G. Gliemann, *J. Lumin.* **1986**, *35*, 261; c) M. Morita, T. Ozawa, T. Tsubomura, *J. Lumin.* **1992**, *53*, 495-498; d) T. Wu, J. Kapitan, V. Andrushchenko P. Bour, *Anal. Chem*. **2017**, *89,* 5043;e) D. H. Metcalf, T.C. VanCott, S.W. Snyder, P. N. Schatz, B.E. Williamson, *J. Phys. Chem.* **1990**, 94, 7, 2828.

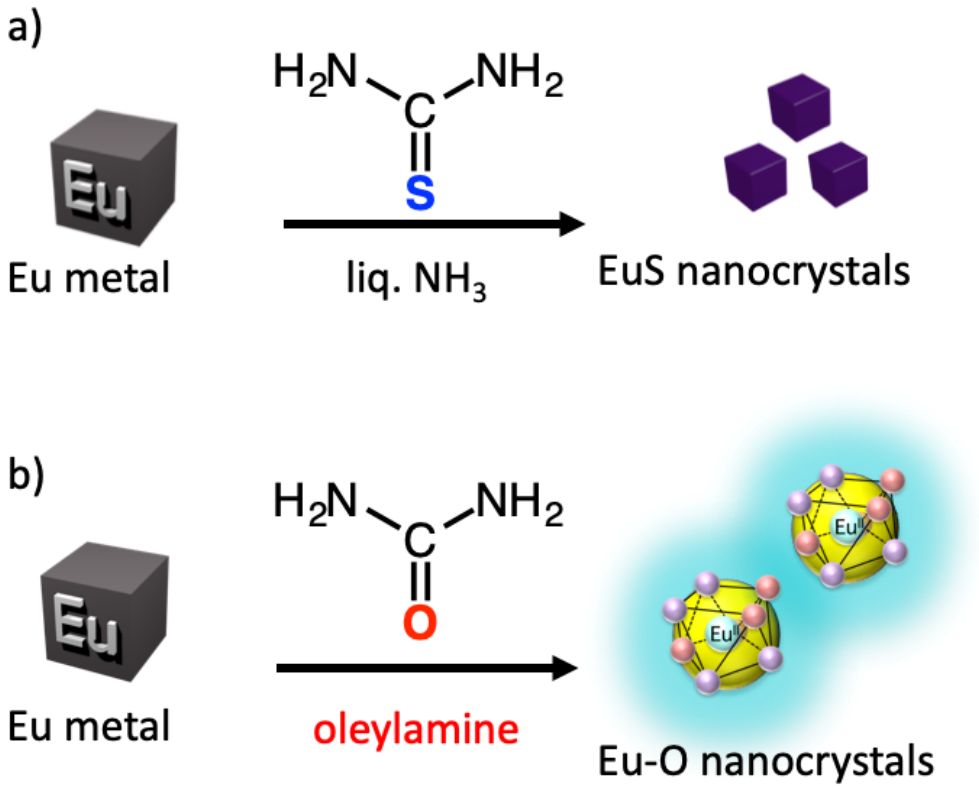

Figure 1. Conceptual synthetic schemes of Eu-S and Eu-O nanocrystals.

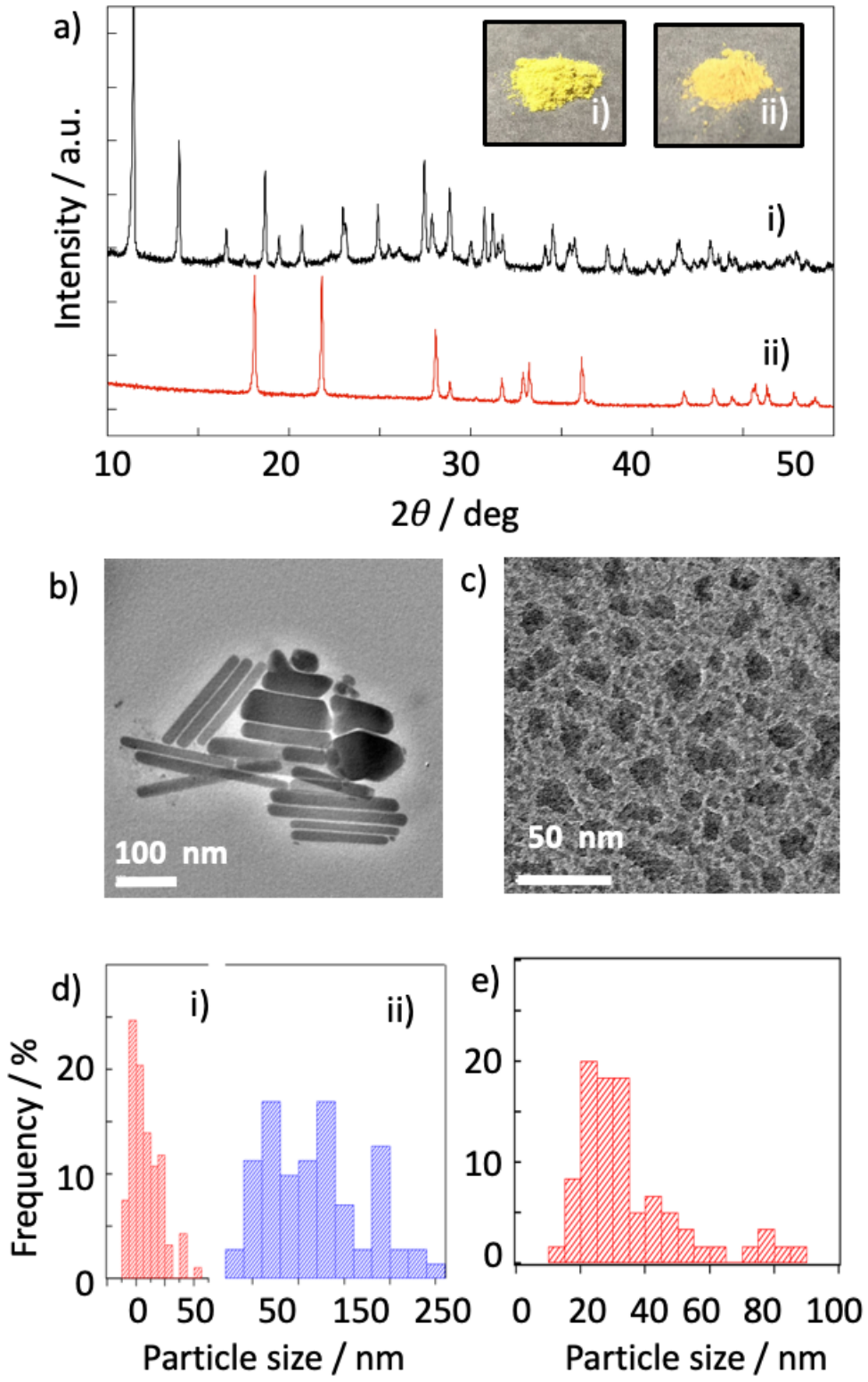

Figure 2. a) XRD profiles of (i) $Eu(OCN)_2$-urea and (ii) $Eu(OCN)_2$ nanocrystals. b) TEM image of $Eu(OCN)_2$-urea nanorods (c) TEM image of $Eu(OCN)_2$ nanocrystals. d) Size distribution of $Eu(OCN)_2$-urea nanorods (i: width of nanorods, ii: length of nanorods). e) Size distribution of $Eu(OCN)_2$ nanocrystals.

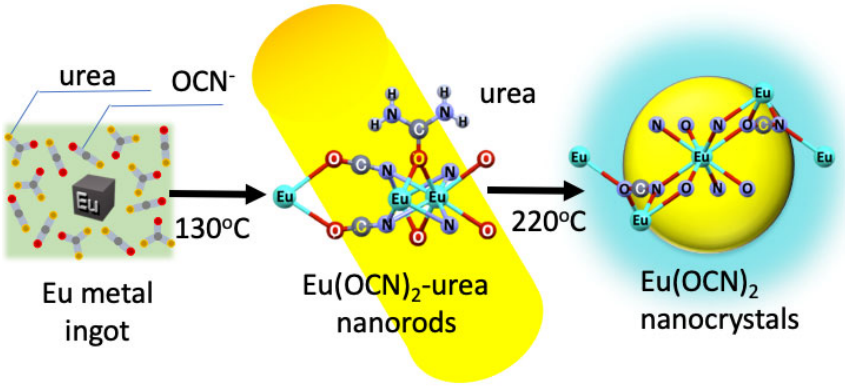

Figure 3. Schematic image of $Eu(OCN)_2$ preparation process

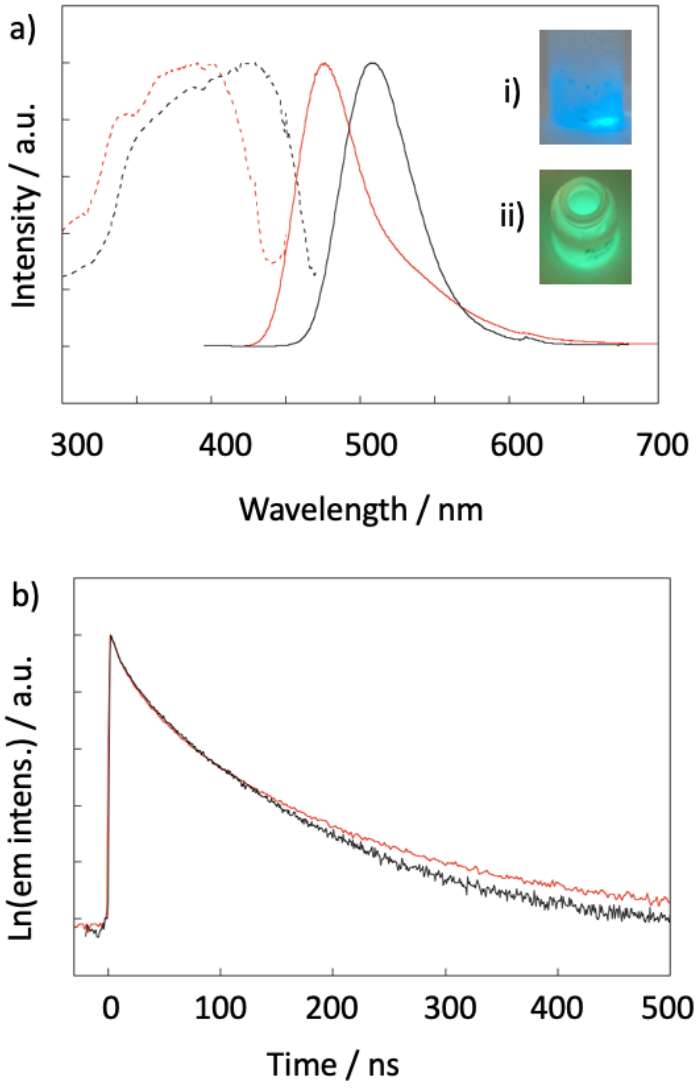

Figure 4. a) Emission and excitation spectra of i) $Eu(OCN)_2$ nanocrystals (red line) and ii) $Eu(OCN)_2$-urea (black line). b) Emission decay profiles of $Eu(OCN)_2$-urea (black line) and (ii) $Eu(OCN)_2$ nanocrystals (red line).

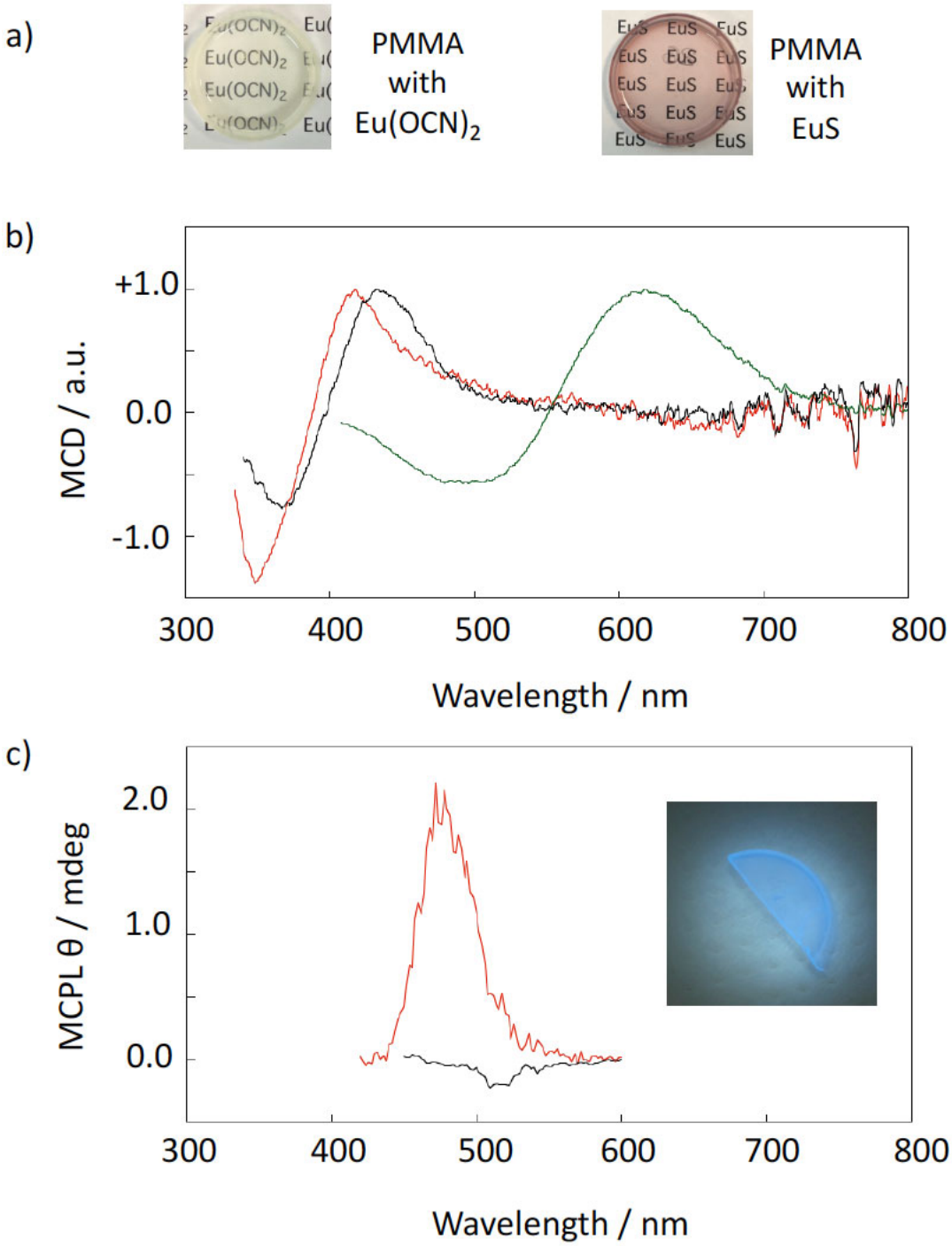

Figure 5. a) Image pictures of PMMA disks containing $Eu(OCN)_2$ and EuS nanocrystals. b) Circularly polarized absorption (CD) spectra of $Eu(OCN)_2$ (red line), $Eu(OCN)_2$-urea (black line) and EuS (green line) nanocrystals under 1.6 T. Concentration of nanocrystals in polymer films:0.5wt%. c) Circularly polarized luminescence (CPL) of PMMA disks containing $Eu(OCN)_2$ (red line) and $Eu(OCN)_2$-urea (black line) under 1.6 T. Inset picture is a luminescent PMMA disk containing $Eu(OCN)_2$ under 100K.

Table 1. Circularly polarized absorption (CD) and emission (CPL) of Eu(II) nanocrystals in PMMA disks.[a)]

Sample	Positive peak wavelength of CD /nm	Dissymmetry factor $g_{M\text{-}CD}$	Emission peak wavelength of CPL /nm	Dissymmetry factor $g_{M\text{-}CPL}$
$Eu(OCN)_2$	410	0.0063	480	0.01
$Eu(OCN)_2$-urea	420	0.0055	520	~0.001
EuS	640	0.0253	non	-

[a)] Circularly polarized absorption (circular dichroism: CD) and luminescence (CPL) of $Eu(OCN)_2$ and $Eu(OCN)_2$-urea were measured under magnetic field (1.6 T) under 100 K.

The table of contents entry should be 50−60 words long and should be written in the present tense and impersonal style (i.e., avoid we). The text should be different from the abstract text.

Keyword Europium, semiconductor, nanocrystal, Circularly polarized luminescence

Yasuchika Hasegawa,* Katsumasa Koide, Makoto Tsurui, Yuichi Kitagawa, Takayuki Nakanishi, Yoshihiro Doi, Yukio, Hinatsu and Koji Fushimi

First circularly polarized absorption and luminescence of semiconductor Eu-OCN nanocrystals in blue light region

Semiconductor nanomaterials with efficient polarized-light control are promising candidates for future photo-information technology and display devices. Novel semiconductor $Eu(OCN)_2$ nanocrystals with circularly polarized absorption (CD) and circularly polarized luminescence (CPL) in the blue light region are reported. This finding may lead to the development of a novel area in the field of polarized-light science and technology.